Journal of Engineering Mathematics **27**: 233–244, 1993.

Spatial stability of the Daniels and Eagles profiles

M.E. MUWEZWA

Mathematics Department, University of Botswana, Gaborone, Botswana, Africa

Received 12 February 1991; accepted in revised form 11 December 1992

Abstract. Daniels and Eagles [1] obtained velocity profiles for exponential slender tubes. The spatial stability of these profiles is examined using a quasi-parallel approach. Contrary to expectation the profiles turn out to be stable.

1. Introduction

We shall be concerned with the stability to small disturbances of the Daniels and Eagles [1] velocity profiles. Daniels and Eagles [1] studied viscous flows in exponential tubes of varying radius. The flows were governed to a first approximation by a nonlinear ordinary differential equation

$$G''' + \frac{1}{\eta} G'' - \frac{1}{\eta^2} G' + 4\gamma GG' = 0\,, \tag{1.1}$$

where $\gamma = \lambda a$, $\lambda = \epsilon \bar{R}$, $H = e^{az}$, $z = \epsilon x$, H is the radius of the tube, $\eta = r/H(z)$, r is the radial coordinate, x is the downstream coordinate, a is a constant, ϵ is a small parameter and $\bar{R}$ is the Reynolds number.

Equation (1.1) will be referred to as the DE equation and the associated solutions as the DE profiles, velocities or flows. The case $\gamma = 0$ corresponds to Poiseuille flow. As γ changes the flows change from Poiseuille flow to other flows. Daniels and Eagles [1] found multiple solutions for both negative and positive values of γ. We consider branch 1 of their solution and carry out stability analysis for γ in the range $|\gamma| \leqslant 6$.

For large values of z, the theory became invalid due to the exponential variation of the radius which was unbounded. This has since been modified and extended by Eagles [2] so that the solution may be applied to a wide variety of 'locally exponential' tubes. He predicted that the DE profiles were good approximations for more general slender tubes. An investigation into approximations to flow in slender tubes by Eagles & Muwezwa [3] confirmed that the DE profiles were good approximations to slender tubes.

Earlier studies by Eagles [4], Eagles and Weissman [5] and Eagles and Smith [6] show that for channel flow, instabilities occurred at $R = 215$ for $\alpha = 0.01$ and $R = 40$ for $\alpha = 0.1$, where α is the semi-divergence angle of the channel. A similar pattern was expected for the DE profiles. The behaviour of the profiles is examined as γ varies by means of spatially growing modes using quasi-parallel stability theory.

2. Stream function equation

The stream function equation is derived from the Navier-Stokes equations with zero external forces

$$\frac{\partial \bar{U}}{\partial t'} + \bar{U} \cdot \nabla \bar{U} = -\frac{1}{\rho} \nabla p + \nu \nabla^2 \bar{U} \tag{2.1}$$

$$\nabla \cdot \bar{U} = 0 \tag{2.2}$$

where $\bar{U}$, ρ and p are the velocity, density and pressure of the fluid respectively, and ν is the kinematic viscosity.

For axisymmetric flows with cylindrical coordinates (r', θ, x') and $\bar{U} = (u', 0, v')$, a stream function may be defined by

$$u' = -\frac{1}{r'} \frac{\partial \psi'}{\partial x'}, \quad v' = \frac{1}{r'} \frac{\partial \psi'}{\partial r'}. \tag{2.3}$$

This satisfies the equation of continuity (2.2). The variables are made non-dimensional as follows:

$$x = \frac{x'}{T}, \quad r = \frac{r'}{T}, \quad \psi = \frac{\psi'}{M}, \quad t = \frac{Mt'}{T^3}, \tag{2.4}$$

where T is the radius of the tube at $x' = 0$ and M is the volumetric flow rate.

The non-dimensional stream function satisfies the equation

$$\frac{1}{r} \frac{\partial D^2 \psi}{\partial t} + \frac{1}{r^2} \left(\psi_r \frac{\partial}{\partial x} - \psi_x \frac{\partial}{\partial r} \right) D^2 \psi + \frac{1}{r^3} (2\psi_x \psi_{xx} + 3\psi_x \psi_{rr} - \psi_r \psi_{rx}) - \frac{3}{r^4} \psi_x \psi_r$$
$$= \frac{1}{\bar{R}} \left(\frac{1}{r} D^4 \psi - \frac{2}{r^2} (\psi_{rxx} + \psi_{rrr}) + \frac{3}{r^3} \psi_{rr} - \frac{3}{r^4} \psi_r \right), \tag{2.5}$$

where $\bar{R} = M/L\nu$ is the Reynolds number and

$$D^2 \equiv \frac{\partial^2}{\partial r^2} - \frac{1}{r} \frac{\partial}{\partial r} + \frac{\partial^2}{\partial x^2}. \tag{2.6}$$

The boundary conditions are

$$\begin{aligned} &\psi = O(r^2) && \text{as } r \to 0, \\ &\psi_r = 0 && \text{at the tube wall}, \\ &\psi = (2\pi)^{-1} && \text{at the tube wall}. \end{aligned} \tag{2.7}$$

The total stream function ψ is considered to be made of two parts, the steady-state and the time-dependent part i.e.

$$\psi(r, x, t) = \hat{F}(r, x) + \hat{\Psi}(r, x, t). \tag{2.8}$$

Daniels and Eagles derived the steady-state stream function equation for flow in tubes of

slowly varying radius by defining the boundary as $r = H(z)$, where $z = \epsilon x$ and ϵ is a small parameter. It is convenient to define a new variable η by

$$\eta = \frac{r}{H(z)}, \tag{2.9}$$

The steady-state stream function $\psi(\eta, z)$ was expanded as follows, since the boundary conditions do not contain ϵ,

$$\psi = \psi_0(\eta, z) + \epsilon^2 \psi_2(\eta, z) + \cdots. \tag{2.10}$$

Substituting into the steady-state equation and defining $\psi_0 = F(\eta, z)$, the $O(1)$ equation for F becomes

$$\mathscr{L}(F) = \lambda\left(4\frac{H'}{H}\left(\frac{1}{\eta^2}(F_\eta)^2 - \frac{1}{\eta}F_\eta F_{\eta\eta}\right) + F_\eta\left(\frac{1}{\eta}F_{\eta\eta z} - \frac{1}{\eta^2}F_{\eta z}\right)\right.$$
$$\left. + F_z\left(-\frac{1}{\eta}F_{\eta\eta\eta} + \frac{3}{\eta^2}F_{\eta\eta} - \frac{3}{\eta^3}F_\eta\right)\right), \tag{2.11}$$

where $\lambda = \epsilon \bar{R}$ and

$$\mathscr{L} \equiv \frac{\partial^4}{\partial\eta^4} - \frac{2}{\eta}\frac{\partial^3}{\partial\eta^3} + \frac{3}{\eta^2}\frac{\partial^2}{\partial\eta^2} - \frac{3}{\eta^3}\frac{\partial}{\partial\eta}, \tag{2.12}$$

with boundary conditions

$$\begin{aligned} &F = O(\eta^2) && \text{as } \eta \to 0, \\ &F = (2\pi)^{-1} && \text{at } \eta = 1, \\ &F_\eta = 0 && \text{at } \eta = 1. \end{aligned} \tag{2.13}$$

The problem for F is called the slender tube problem and will constitute our basic flow.

For exponential tubes with $H = e^{az}$, where a is a constant, a solution independent of z is allowable and we obtain the nonlinear ordinary differential equation (1.1) with G defined by

$$G = \frac{1}{\eta}F_\eta. \tag{2.14}$$

The DE flows are not just small perturbations of Poiseuille flow, but the first constitute a family of flows containing not only Poiseuille flow but also flows with inflexion points and with regions of reversed flow.

3. Disturbance equation

It is known that Poiseuille flow is stable to small axisymmetric disturbances for all Reynolds numbers, the observed instabilities being attributed to finite amplitude effects. Many slender

channel flows have been shown to be unstable for sufficiently high values of the parameter $\gamma = \lambda H'/H$. A similar behaviour was expected for slender tubes.

To study a small disturbance ψ to the basic steady flow F we superimpose the disturbance on the basic flow so that the total stream function is given by

$$\psi = F(\eta, z) + \Psi(\eta, x, t)\,. \tag{3.1}$$

Substituting ψ into equation (2.5) and linearising we obtain to $O(1)$ the disturbance equation

$$\begin{aligned} &H^2\eta^3\Psi_{\eta\eta t} + H^4\eta^3\Psi_{xxt} + \eta^2 F_\eta \Psi_{\eta\eta x} + H^2\eta^2 F_\eta \Psi_{xxx} \\ &\quad - H^2\eta^2\Psi_{\eta t} + (-\eta^2 F_{\eta\eta\eta} + 3\eta F_{\eta\eta})\Psi_x - \eta F_\eta \Psi_{\eta x} - 3F_\eta \Psi_x \\ &\quad = \frac{1}{\bar{R}}(\eta^3\Psi_{\eta\eta\eta\eta} + 2H^2\eta^3\Psi_{\eta\eta xx} + H^4\eta^3\Psi_{xxxx} - 2H^2\eta^2\Psi_{\eta xx} - 2\eta^2\Psi_{\eta\eta\eta} + 3\eta\Psi_{\eta\eta} - 3\Psi_\eta)\,, \end{aligned} \tag{3.2}$$

with boundary conditions

$$\Psi(1, x) = \Psi_\eta(1, x) = 0\,, \tag{3.3}$$

and

$$\Psi(0, x) = \Psi_\eta(0, x) = 0\,, \tag{3.4}$$

is the regularity condition at the center. Note that the coefficients of the equation will now vary slowly with z in view of the slow variable $z = \epsilon x$. The coefficients of the disturbance are independent of time, it contains time only through the derivatives with respect to t. Therefore we look for constant frequency solutions of the form

$$\Psi = \phi(\eta, z)\, \mathrm{e}^{\mathrm{i}(S(X) - \beta t)} + \text{C.C.}\,, \tag{3.5}$$

where

$$\frac{\mathrm{d}s}{\mathrm{d}x} = K(z)\,, \tag{3.6}$$

C.C. is the complex conjugate and

$$\phi = \phi^{(0)} + \epsilon\phi^{(1)} + \epsilon^2\phi^{(2)} + \epsilon^3\phi^{(3)} + \cdots\,. \tag{3.7}$$

Substituting the solution (3.5) into equation (3.2) we obtain to $O(1)$ the equation

$$\left[R^{-1}(L - q^2)^2 - \mathrm{i}q\left(\left(G - \frac{\omega}{q}\right)(L - q^2) - \eta\left(\frac{G'}{\eta}\right)'\right)\right]\phi = 0\,, \tag{3.8}$$

where

$$R = \bar{R}/H\,, \quad \omega = \beta H^3\,, \quad q = KH\,, \tag{3.9}$$

are the local Reynolds number, frequency and wave number respectively, and

$$L \equiv \frac{\partial^2}{\partial\eta^2} - \frac{1}{\eta}\frac{\partial}{\partial\eta}\,. \tag{3.10}$$

The boundary conditions on ϕ are

$$\begin{aligned} &\phi = \phi_\eta = 0 \quad \text{at } \eta = 0\,, \\ &\phi = \phi_\eta = 0 \quad \text{at } \eta = 1\,. \end{aligned} \tag{3.11}$$

Equation (3.8) represents a sequence of differential equations of which the $O(1)$ equation is the familiar Orr-Sommerfeld equation. We shall be concerned mainly with the solutions of the Orr-Sommerfeld equation written here as

$$(L-q^2)^2\phi^{(0)} - \mathrm{i}qR\left(\left(G-\frac{\omega}{q}\right)(L-q^2) - \eta\left(\frac{G'}{\eta}\right)'\right)\phi^{(0)} = 0\,, \tag{3.12}$$

with boundary conditions

$$\begin{aligned} &\phi^{(0)} = \phi_\eta^{(0)} = 0 \quad \text{at } \eta = 0\,, \\ &\phi^{(0)} = \phi_\eta^{(0)} = 0 \quad \text{at } \eta = 1\,. \end{aligned} \tag{3.13}$$

In other words we shall be using the usual quasi-parallel assumption for studying the stability, and to obtain this approximation we must treat R in the disturbance equation as $O(1)$, even though the base flow was derived on the basis of $R = O(\epsilon^{-1})$. This feature is common in most quasi-parallel stability analysis but it is argued in Eagles & Weissman that the method is allowable, and produces accurate results at least for channel flows.

4. Orr-Sommerfeld equation

The solution of the Orr-Sommerfeld equation for specified real ω and R gives a complex eigenvalue q and a complex eigenfunction. In general, the equation will have four linearly independent solutions, so that

$$\phi^{(0)} = A_1\phi_1 + A_2\phi_2 + A_3\phi_3 + A_4\phi_4 \tag{4.1}$$

where A_i are arbitrary constants and ϕ_i are independent solutions. A series solution of (3.12) enabled us to eliminate immediately those solutions which are not regular near the center of the tube. A linear combination of the remaining solutions yielded

$$\phi^{(0)} = A_1\phi_1 + A_2\phi_2\,. \tag{4.2}$$

By applying the boundary conditions (3.13) we obtained two homogeneous equations for the constants A_1 and A_2. For a non-trivial solution to exist the determinant of the coefficients A_1 and A_2 must vanish, leading to

$$F(R, \omega, q) = \phi_1(1)\phi_2'(1) - \phi_1'(1)\phi_2(1) = 0\,. \tag{4.3}$$

The eigenvalues q must be determined for selected real positive values of R and ω. If $q = q_r + \mathrm{i}q_i$, q_i determines whether or not the basic flow is stable to small disturbances. If q_i is positive the flow is considered to be stable. If it is negative the flow is unstable. The case $q_i = 0$ indicates neutral stability. In general a number of types of modes are possible each

with a spectrum of eigenvalues, (See Drazin and Reid [7]). Searching for the least stable or unstable eigenvalue is by no means an easy task.

On expanding equation (3.12) we obtain

$$(\eta^4 D^4 - 2\eta^3 D^3 + (3 - A\eta^2)\eta^2 D^2 + (-3 + A\eta^2)\eta D + (B + iqRU)\eta^4)\phi^{(0)} = 0\,, \tag{4.4}$$

where

$$\begin{aligned} D &= \frac{\mathrm{d}}{\mathrm{d}\eta}\,, \\ A &= 2q^2 + iqR\left(G - \frac{\omega}{q}\right), \\ B &= q^4 + iq^3 R\left(G - \frac{\omega}{q}\right), \\ U &= \eta\left(\frac{G'}{\eta}\right)', \end{aligned} \tag{4.5}$$

with boundary conditions $\phi^{(0)}, \phi_\eta^{(0)}$, regular at $\eta = 0$ and $\phi^{(0)}(1) = \phi_\eta^{(0)}(1) = 0$, on the walls. The velocity function $G(\eta)$ was defined in (2.14) for the DE profiles. The following alternative form from Eagles and Muwezwa [3] was more convenient to use for the series solution in powers of η which will be used for small values of η to start the Runge-Kutta Scheme;

$$G = 2\sum_{k=1}^{8} (-1)^{k+1} k g_k \eta^{2k-2}\,, \tag{4.6}$$

$$U = 8\sum_{k=1}^{\infty} k(k-1)(k-2) g_k (-1)^{k+1} \eta^{2k-4}\,, \tag{4.7}$$

where $(-1)^{k+1} g_k$ are the coefficients of η^{2k} in the expansion of F.

Equation (4.4) is an ordinary differential equation which may be solved by the Frobenius method. Let

$$\phi^{(0)} = \sum_{r=0}^{\infty} A_r \eta^{s+r}\,. \tag{4.8}$$

On substituting the series into (4.4) we obtain a series solution with four arbitrary constants,

$$\phi^{(0)} = A_0(1 + \cdots) + A_1(\eta^2 + \cdots) + A_2(\eta^4 + \cdots) + A_3(\eta^2 \log \eta + \cdots) \tag{4.9}$$

The boundary conditions at the center of the tube require that A_0 and A_3 are both zero. The appropriate solution that satisfies the boundary conditions is given by

$$\phi^{(0)} = A_1\phi_1 + A_2\phi_2\,, \tag{4.10}$$

where for small values of η

$$\phi_1 = \eta^2 - \frac{1}{192} Q\eta^6 + \frac{1}{1152}\left(M - \frac{1}{8} PQ\right)\eta^8 + \cdots\,, \tag{4.11}$$

$$\phi_2 = \eta^4 + \frac{8}{192} P\eta^6 + \frac{1}{1152}(P^2 - Q - N)\eta^8 + \cdots , \tag{4.12}$$

$$P = 2q^2 + \mathrm{i}qR\left(2g_1 - \frac{\omega}{q}\right),$$

$$Q = q^4 + \mathrm{i}q^3R\left(2g_1 - \frac{\omega}{q}\right), \tag{4.13}$$

$$M = 4\mathrm{i}qR(g_2q^2 - 12g_3),$$

$$N = \mathrm{i}qR(32g_2).$$

This series was used to calculate the starting values for the Runge-Kutta integration scheme. The fourth-order Runge-Kutta routine in double precision was used for all calculations to minimise both truncation and roundoff errors. A step length of 1/20 was used throughout with some numerical checks made on a step length of 1/40.

5. Numerical solution

The Orr-Sommerfeld equation was considered in the form

$$\eta^4\phi^{iv} = 2\eta^3\phi''' - \eta^2 y_1\phi'' - \eta y_2\phi' - y_3\phi , \tag{5.1}$$

where

$$y_1 = 3 - A\eta^2 ,$$

$$y_2 = -y_1 ,$$

$$y_3 = (B + \mathrm{i}qRU)\eta^4 . \tag{5.2}$$

The equation was integrated in double precision from 0.05 to 1 in view of the singularity at $\eta = 0$, the series solution (4.10) being used up to $\eta = 0.05$. For the solution $\phi^{(0)} = A_1\phi_1 + A_2\phi_2$, the computer considered two stages initially to obtain two independent solutions. The stages are: $A_1 = 1$, $A_2 = 0$ and $A_1 = 0$, $A_2 = 1$. Later an attempt was made to satisfy the boundary conditions at $\eta = 1$. At each stage integration proceeded using a fourth-order Runge-Kutta procedure evaluating ϕ, ϕ', ϕ'', and ϕ''' until $\eta = 1$. These values were stored. The stored values were used to obtain the eigenvalue relation.

$$F(R, \omega, q) = \phi_1(1)\phi_2'(1) - \phi_1'(1)\phi_2(1) = 0 . \tag{5.3}$$

For fixed values R and ω, the eigenvalues of q must be found by searching iteratively for the zeroes of F. In order to effect the procedure we needed the values of R, ω and needed a good estimate of q.

Although the above procedure is simple its numerical implementation can lead to serious difficulties especially when R is large. The difficulty arises from the fact that although the solutions ϕ_1 and ϕ_2 are numerically satisfactory near $\eta = 0$, they both contain some multiple of the rapidly growing viscous solution and causes loss of linear independence near $\eta = 1$.

One of the methods of overcoming this difficulty, proposed by Nachtsheim [8], is based on the method of matched initial-value problems. In this method, in addition to forward integration from $\eta = 0$, a backward integration is also made from $\eta = 1$ and the eigenvalue relation is then obtained by matching the results at an interior point of the interval, e.g. the midpoint. Other methods for dealing with this difficulty include filtering as in Kaplan [9].

In the present study R was first kept reasonably low at $R = 40$ and the frequency was fixed at $\omega = 1$. The search was made by plotting contour lines $F_r = 0$, $F_i = 0$ in the complex q-plane, where F_r and F_i are the real and imaginary parts of F. Any intersection of the contour lines $F_r = 0$ and $F_i = 0$ indicate the approximate location of a root. A typical contour plot is shown in Fig. 1 for the first and fourth quadrants. The approximate root found in this way was used as an estimate for the eigenvalue q. A more accurate value was obtained by a root finding routine based on successive linear interpolation. In the range $-10 \leq q_r \leq 10$ and $-4 \leq q_i \leq 4$ no unstable roots were found for $R = 40$, $\omega = 1$ at both $\gamma = 0$ and $\gamma = 6$. Two stable roots were found in the first quadrant, of which the least stable root is shown in Fig. 1. The second root was also confirmed by an independent program used by Eagles (Private communication). The roots were determined by the root finding routine at $\gamma = 0$, $R = 40$,

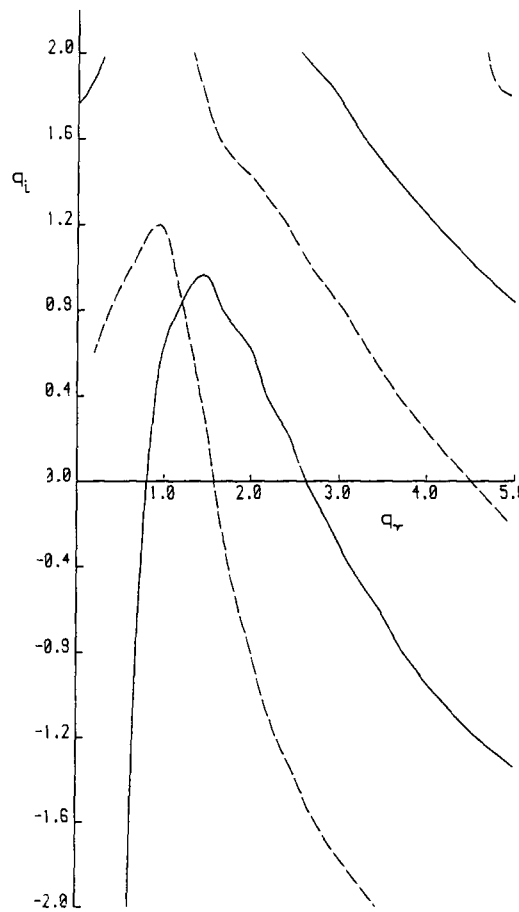

Fig. 1. Contour plot of least stable eigenvalue for $\gamma = 6$, $R = 40$ and $\omega = 1$. $-F_r$; $-F_i$.

$\omega = 1$ as $q_1 = (1.74916, 1.32565)$ and $q_2 = (1.82435, 3.34520)$. In the next section we look at the behaviour of the least stable eigenvalue as R, ω and γ are varied.

6. Least stable eigenvalue

We next considered values of $\gamma > 0$. The contour plots and the root finding routine found no unstable eigenvalues in the region $-10 \leq q_r \leq 10$ and $-4 \leq q_i \leq 4$ for $R = 40$, $\omega = 1$ at various values of γ up to 6. Extensive checks were made on the programs and the contour plots are quite reliable in revealing possible locations of the eigenvalues. The eigenvalues found in the first quadrant were also confirmed by an independent program.

An alternative to finding an eigenvalue with q_i negative was to study the behaviour of the least stable eigenvalue as γ, R and ω are varied. In Fig. 2, we show the variation of the eigenvalue with γ at $R = 40$ and $R = 60$. The eigenvalue becomes less stable with increasing R and γ as expected. However, this trend slows down with increasing R and exhibits a tendency to level at about $R = 400$. This behaviour is well indicated in Fig. 4 where q_i begins to level around $R = 210$. A scatter diagram of the eigenvalue at various values of R is given in Fig. 3. It is interesting to note that the least stable root remains stable at Reynolds numbers as high as $R = 450$ at $\gamma = 6.6$.

The variation of q_i with ω is shown in Fig. 5. Despite that the changes are made at $\gamma = 6.6$ for $R = 200$ and $R = 300$, the eigenvalue remains stable. The results given are merely a

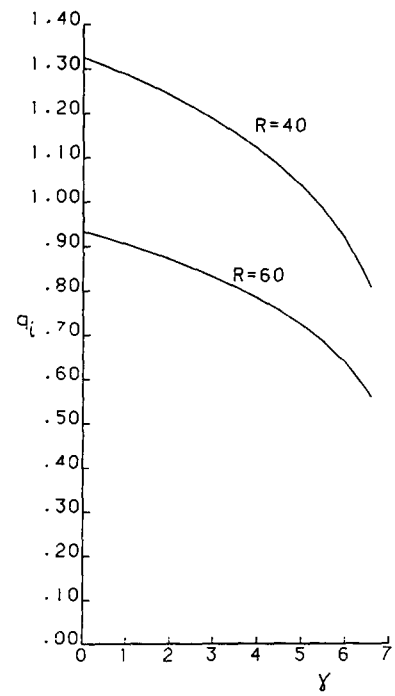

Fig. 2. Variation of q_i with γ at $R = 40$ and $R = 60$ for $\omega = 1$.

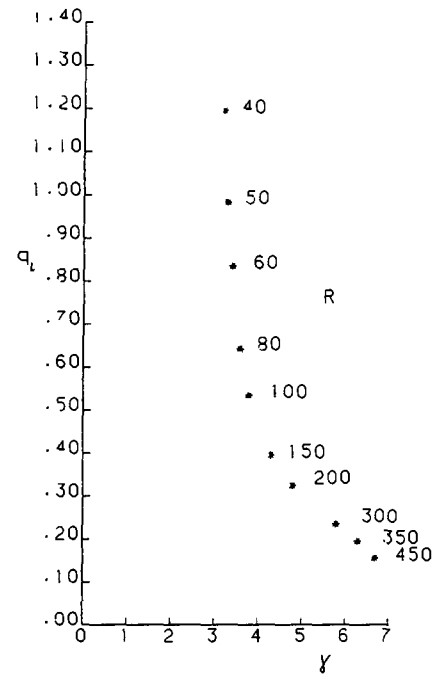

Fig. 3. q_t at various values of γ and R, $\omega = 1$.

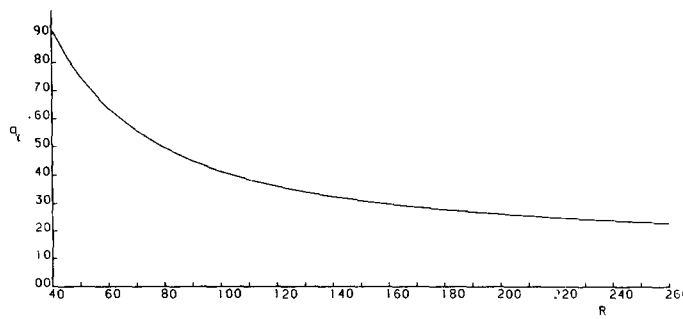

Fig. 4. Variation of q_t with R for $\gamma = 6$ and $\omega = 1$.

section of an extensive study which was made on similar lines. No evidence was found of roots with negative q_t for $-6 \leq \gamma \leq 6$, $0 \leq R \leq 500$, and $0 \leq \omega \leq 1$.

Conclusions

The stability of the DE profiles has been investigated by quasi-parallel theory. All cases investigated were stable, but stability decreases with increasing values of γ and R. Contour plots were used in the search for eigenvalues in the complex q − plane. Two eigenvalues were found at $\gamma = 0$, $R = 40$ and $\omega = 1$ of which the least stable is $q = (1.74916, 1.32565)$.

Stability tests were carried out on q by varying γ, R and ω. No instability was found for $|\gamma| \leq 6$, $R < 500$ and $\omega \leq 1$. In Fig. 2 the variation of q_t with γ at fixed values of R, shows that stability decreases with increasing values of γ and R. As a result one would have

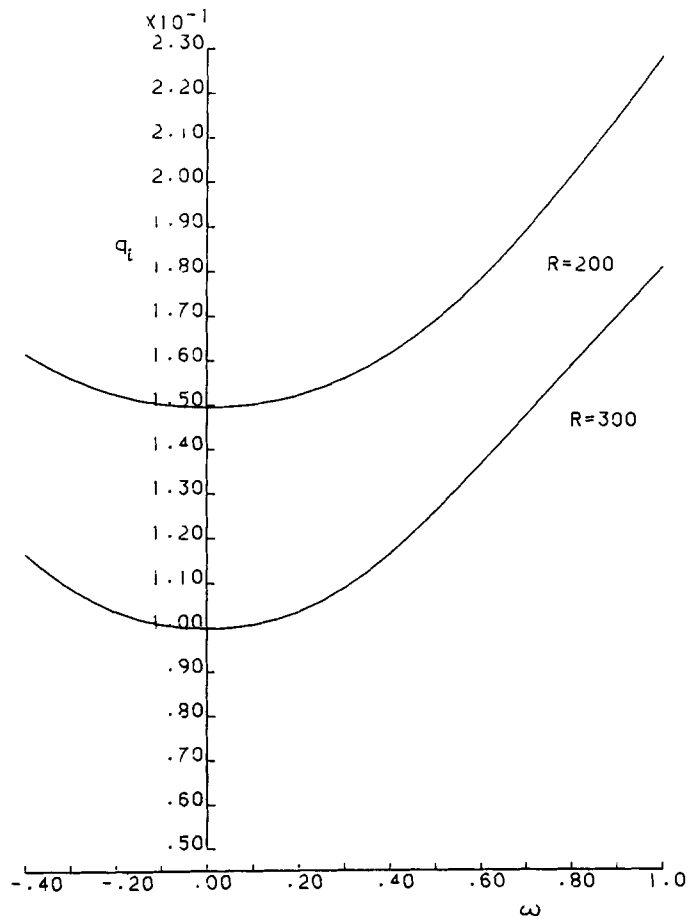

Fig. 5. Variation of q_i with ω at $\gamma = 6.6$ for $R = 200$ and $R = 300$.

expected the root to be unstable if γ was fixed at $\gamma = 6$ while R was increased but this was not the case. Instead the root remained stable even for R as high as 260. The variation of q_i with ω at $\gamma = 6.6$ for $R = 200$ and $R = 300$ is an interesting case. Here the curves are parabolic and symmetrical about q_i-axis, showing that for fixed R the root becomes more stable as ω increases in the positive direction and decreases in the negative direction. Nevertheless, stability still decreases with higher values of R even though the eigenvalue does not become unstable.

References

1. P.G. Daniels and P.M. Eagles, High Reynolds number flows in exponential tubes of slow variation. *J. Fluid Mech.* **90** (1979) 305.
2. P.M. Eagles, Steady flow in locally exponential tubes. *Proc. R. Soc. Lond.* A. 383 (1982) 231.
3. P.M. Eagles and M.E. Muwezwa, Approximations to flow in slender tubes. *J. Eng. Math.* **20** (1986) 51.
4. P.M. Eagles, The stability of Jeffery-Hamel solutions for divergent channel flow. *J. Fluid Mech.* **24** (1966) 191.
5. P.M. Eagles and M.A. Weissman, On the stability of slowly varying flow: the divergent channel. *J. Fluid Mech.* **69** (1975) 241.

6. P.M. Eagles and F.T. Smith, The influence of nonparallelism in channel flow stability. *J. Eng. Math.* **14** (1980) 219.
7. P.G. Drazin and W.H. Reid, *Hydrodynamic Stability*. Cambridge University Press (1982).
8. P.R. Nachtsheim, An initial value method for the numerical treatment of the Orr-Sommerfeld equation for the case of plane Poiseuille flow. *Nat. Aero. Space Admin. Tech.* Note No. D-2414 (1964)
9. R.E. Kaplan, *The stability of laminar incompressible boundary layers in the presence of compliant boundaries.* Aero-elastic and Structures Research Laboratory, Massachusetts Institute of Technology. Report No. ASLR-TR 166-1 (1964).